

# The phenomenology of fluctuation induction

A. S. Zel'tser and A. É. Filippov

Donetsk Physicotechnical Institute, Ukrainian Academy of Sciences, 340114 Donetsk, Ukraine

(Submitted 24 January 1994)

Zh. Eksp. Teor. Fiz. **106**, 1117–1135 (October 1994)

We analyze the phenomenon of induction of first-order phase transitions (PT1) by large-scale critical fluctuations from the viewpoint of the kinetics of the nucleation process. We show that although the local density of the free energy functional of the system is such that, in accordance with the Landau theory, the system should undergo a continuous phase transition (a second-order phase transition, or PT2), under certain conditions the interaction of fluctuations gives rise to ordered-phase nuclei typical of PT1. We reveal how the separatrices isolating the PT1 and PT2 regions on the phase portrait of the renormalization-group equations correlate with the different versions of the ordering kinetics. © 1994 American Institute of Physics.

## 1. INTRODUCTION

The problem of the critical behavior of systems near the points and curves of second-order phase transitions (PT2) has been in the foreground for a long time. The main difficulty in studying such systems is that in this region the fluctuations of the order parameter not only are small in comparison with the average value of the order parameter but also interact strongly with one another, so that at the critical point proper their correlation range tends to infinity. Kadanoff's idea,<sup>1</sup> motivated by this, of using scaling transformations and the renormalization-group (RG) method, based on these transformations and developed by Wilson,<sup>2,3</sup> have made it possible to move far ahead in describing critical behavior. Especially impressive achievements have been made in calculating critical exponents, which characterize the degree to which thermodynamic quantities diverge at the critical point.<sup>3–5</sup> A secondary and somewhat unexpected result of the fluctuation theory of critical phenomena was the discovery that fluctuations may greatly affect the way in which phase transitions occur. We discuss this possibility in greater detail.

The hypothesis of the scaling invariance of a system at the PT2 point, employed within the RG method, assumes that the parameters of the Ginzburg–Landau–Wilson (GLW) functional renormalized owing to the fluctuation interaction, reach the stable fixed point of the RG equations in the limit. This is indeed the case when we are dealing with a model problem with a fluctuating scalar field  $\varphi$  or an isotropic model with a vector  $n$ -component field  $\varphi = \{\varphi_i\}$ . But as soon as the system becomes slightly more complicated (i.e., when there appear various invariants composed of the  $\varphi_i$  or when there is interaction between order parameters of disparate nature), the phase portrait of the RG equations separates into regions in which the phase trajectories starting at some of them do not end at the stable fixed point but leave the limits of positive definiteness of the quaternary form in the GLW functional. Occasionally there is no stable fixed point, and no matter where the trajectories begin they leave the region of stability of the partition function calculated with the given form of GLW. These properties of RG equations were discovered early in the application of the method and then were repeatedly corroborated in attempts to apply the RG method

to various physical systems (see, e.g., Refs. 6–14 and the literature cited in the review articles of Refs. 15–17).

The fact that the phase trajectories leave the stability region explicitly contradicted the initial hypothesis of the RG method and required stepping outside the limits of the method. The first obvious idea is that terms of the form  $\varphi^6$  should be kept when the quaternary form changes sign. This ensures that the partition function again becomes convergent and the phase transition is of the PT1 type. Such augmenting of the GLW functional makes the functional unrenormalizable in the sense of the theory of fields,<sup>18</sup> where the RG method actually originated in its traditional form, so that it seemed that the standard approach was not applicable. However, the RG equations can be left unchanged, while the effective functional of the system free energy near the stability limits is calculated in a more meaningful way, retaining its positive definiteness as  $|\varphi| \rightarrow \infty$ . Various researchers have performed such computations using the ring approximation and by employing models that allow for an exact calculation of the partition function (see, e.g., Refs. 19–23), and confirmed the hypothesis of induction of PT1. A fundamental drawback of such approaches is that calculations of the effective GLW functional rest on “small” parameters that actually are not small or on entirely unmanageable approximations.

Another possibility that cannot be discarded offhand is that this behavior of the trajectories (their leaving the stability region) originates in the mathematically improper expansion in powers of the quantity  $\varepsilon = 4 - d$ , which is actually not small at all, where  $d$  is the dimensionality of the space (here  $\varepsilon = 1$  for  $d = 3$ ).<sup>2,3</sup> However, calculations based on the exact RG equation<sup>24–27</sup> have shown that the assumption that the vertices of the GLW functional are small, used in the  $\varepsilon$ -expansion, can be supported by the real smallness of the respective quantities for the physical branch of the solution of this equation.<sup>25</sup> More than that, applying the exact RG equation to anisotropic systems yields the same arrangement of the separatrices in the phase portrait as using the  $\varepsilon$ -expansion.<sup>24,27</sup>

To clarify the phenomenology of fluctuation induction of PT1, an assumption about the specific spatial structure of the  $\varphi$ -field in the critical region was made. More precisely, it

was assumed that the system contains large-scale (mesoscopic) nonlinear excitations that in appropriate conditions may act as critical (and supercritical) nuclei of the new phase,<sup>28</sup> which is typical of PT1 phenomenology (see Ref. 29). Although in itself the qualitative picture of the structured nature of the  $\varphi$ -field in the vicinity (and in the process) of the transition is, apparently, true and is corroborated by numerical modelling of both PT2 and PT1 (see Refs. 30–32), calculations of the effective form of the GLW functional again required approximations that are not properly justified and cannot be considered completely satisfactory.

The approach based on the model calculation of the effective free energy is actually a compromise because it is equivalent to the statement that the effective “renormalized” energy is what it should be in the mean-field theory for PT1. The true mechanism of the effect of fluctuations is masked and practically remains an enigma. Indeed, if in PT1 the main reason for nucleation is the presence of an energy barrier in the local GLW-functional density that separates the disordered state from the ordered, then how does nucleation emerge in the critical region where there is no such barrier? This paper is devoted to finding an answer to this question.

For the sake of definiteness we restrict our discussion to the case of two interacting order parameters. Besides being simple from the standpoint of mathematics and relatively transparent, this case is interesting because it can be used to describe the situation, fairly often encountered, in which two transition curves on the phase diagram intersect.<sup>7</sup> In addition, at certain values of the parameters the respective GLW functional describes the behavior of a system with tetragonal symmetry and a two-component order parameter. Finally, similar behavior is observed in the phase transition to superconductivity, which because of the interaction of the two-component superconducting order parameter and the fluctuations of the gauge electromagnetic field is a fluctuation-induced PT1 (Ref. 33).

Since understanding the content of the present paper requires information contained in previous studies within the RG method, for the sake of coherence of exposition we briefly survey the pertinent equations and results, after which we compare them with the results obtained within the kinetic approach.

## 2. THE GLW FUNCTIONAL, THE MEAN-FIELD THEORY, AND THE RG EQUATIONS

The simplest GLW functional for two interacting fluctuating fields is

$$\begin{aligned} \mathcal{A}[\varphi_1; \varphi_2] &= \frac{1}{2} \int d^d r \left[ (\text{grad} \varphi_1)^2 + (\text{grad} \varphi_2)^2 + \tau_1 \varphi_1^2 + \tau_2 \varphi_2^2 \right. \\ &\quad \left. + \frac{1}{2} u_1 \varphi_1^4 + \frac{1}{2} u_2 \varphi_2^4 + v \varphi_1^2 \varphi_2^2 \right] \\ &= \int d^d r \left\{ \frac{1}{2} [(\text{grad} \varphi_1)^2 + (\text{grad} \varphi_2)^2] \right. \\ &\quad \left. + F(\varphi_1; \varphi_2) \right\}. \end{aligned} \quad (1.1)$$

Before investigating fluctuation effects, we give the main results of the Landau theory. Actually, analysis within this theory amounts to studying the shape of the surface  $F(\varphi_1; \varphi_2)$  as a function of the system parameters. To this end it has proved convenient to introduce new parameters:  $\tau = \tau_1 + \tau_2$  and  $\theta = \tau_1 - \tau_2$ . The transition to the ordered phase corresponds to the appearance of nontrivial minima, which occur on the lines  $\tau = \pm \theta$  in the  $\tau \geq 0$  range. If the  $\tau_i$  are below these lines, the structure of the surface  $F(\varphi_1; \varphi_2)$  depends largely on the relationship between the constants in functional (1.1). When there is strong coupling between the fields, with  $v^2 \geq u_1 u_2$ , the minima of  $F(\varphi_1; \varphi_2)$  are located at the points with  $(\varphi_1 \neq 0, \varphi_2 = 0)$  and  $(\varphi_1 = 0, \varphi_2 \neq 0)$ , so that here the Landau theory predicts two possible phases, the transition between which is a PT1 and takes place on the straight line

$$(\sqrt{u_1} - \sqrt{u_2})\tau + (\sqrt{u_1} + \sqrt{u_2})\theta = 0. \quad (1.2)$$

When  $v^2 < u_1 u_2$ , a mixed phase with  $\varphi_2 \neq 0$  and  $\varphi_1 \neq 0$  is possible, and transitions between ordered phases are continuous and take place on the straight lines

$$(u_1 - v)\tau - (u_1 + v)\theta = 0, \quad (u_2 - v)\tau - (u_2 + v)\theta = 0. \quad (1.3)$$

We are interested in the situation in which both temperatures,  $\tau_1$  and  $\tau_2$ , are close to critical, so that both fields,  $\varphi_1$  and  $\varphi_2$ , strongly fluctuate. In accordance with the convention of the RG method, the parameters of the functional (1.1) become renormalized in the critical region, described, respectively, by the RG equations. Since the qualitative effects of interest appear even in the local approximation of RG, that is, in the approximation that ignores the generation of non-local corrections to the GLW functional, we can limit ourselves to the appropriate version of the exact RG equation for  $F(\varphi_1; \varphi_2)$  (Ref. 25):

$$\begin{aligned} \frac{\partial F(\varphi_1; \varphi_2)}{\partial l} &= dF(\varphi_1; \varphi_2) - \sum_{i=1}^2 \left[ (d-2)\varphi_i \right. \\ &\quad \times \frac{\partial F(\varphi_1; \varphi_2)}{\partial \varphi_i} + \frac{\partial^2 F(\varphi_1; \varphi_2)}{\partial \varphi_i^2} \\ &\quad \left. - \left( \frac{\partial F(\varphi_1; \varphi_2)}{\partial \varphi_i} \right)^2 \right], \end{aligned} \quad (1.4)$$

where  $l$  is the renormalization-group time, and  $d$  the dimensionality of the space. The equation is nonlinear and can be solved only numerically. Here renormalization involves not only the fourth-order vertices in (1.1) but also the higher-order vertices generated in the RG transformations. Having in mind comparison of the results of various approaches and the fact that numerical solution of Eq. (1.4) and the standard approach<sup>15–17</sup> yield similar results,<sup>25</sup> we reduce this equation, following Ref. 17, to a system of equations for  $\tau_{1,2}$ ,  $u_{1,2}$ , and  $v$ . In the first  $\varepsilon$ -approximation the system can be written as

$$\frac{\partial \tau_{1,2}}{\partial l} = 2\tau_{1,2} + 3u_{1,2} + v - \tau_{1,2}^2, \quad (1.5)$$

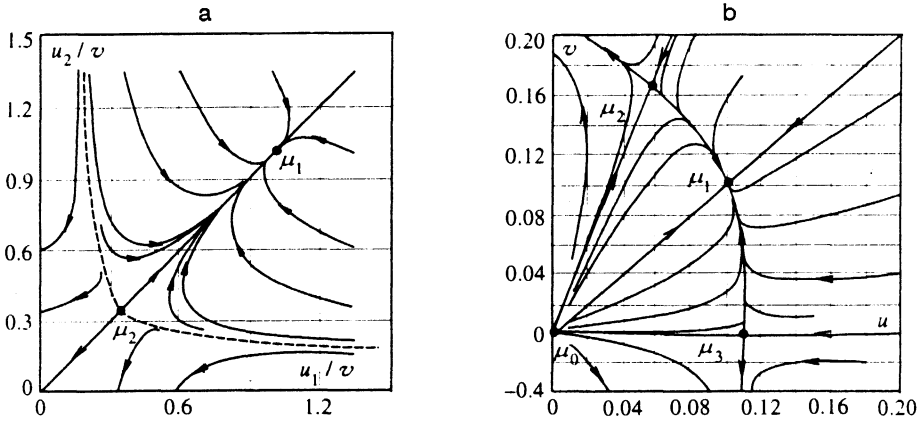


FIG. 1. The phase portrait of the RG equations: (a) in normalized units  $x = u_1/v$  and  $y = u_2/v$ , and (b) in the  $u_1 = u_2 = u$  plane.

$$\frac{\partial u_{1,2}}{\partial l} = \varepsilon u_{1,2} - \frac{9}{2} u_{1,2}^2 - \frac{1}{2} v^2, \quad (1.6)$$

$$\frac{\partial v}{\partial l} = v \left[ \varepsilon - \frac{3}{2} (u_1 + u_2) - 2v \right].$$

Equation (1.5) separates from the other equations and determines the renormalization of  $\tau_{1,2}$ , while the system of equations (1.6) can be solved independently. Since the physically essential quantities are not the quantities  $u_{1,2}$  and  $v$  themselves but their ratios,<sup>7</sup> this system can be simplified further by reducing it to two equations for the ratios  $u_1/v = x$  and  $u_2/v = y$ :

$$\frac{1}{v} \frac{\partial x}{\partial l} = \frac{1}{2} (-6x^2 + 3xy + 4x - 1), \quad (1.7)$$

$$\frac{1}{v} \frac{\partial y}{\partial l} = \frac{1}{2} (-6y^2 + 3xy + 4y - 1).$$

The phase portrait of this system of equations is depicted in Fig. 1a, where  $\mu_{1,2}$  stand for the fixed points,

$$\mu_1: x = y = \frac{1}{3}, \quad \mu_2: x = y = 1, \quad (1.8)$$

and the broken trace represents the separatrix isolating the region where the phase trajectories arrive at the stable fixed point  $\mu_1$  from the region where they leave the limits of positive definiteness of the quaternary form ( $u_1 = 0$  and  $u_2 = 0$ , respectively). Clearly, in both cases the phase trajectories usually approach the curve  $u_1 = u_2$ , and at the stable point  $\mu_1$  the symmetry of the system grows to  $O_2$ . The phenomenon is known as asymptotic symmetry,<sup>16</sup> and in the next section we discuss its kinetic manifestations. The equality  $u_1 = u_2$  also raises the symmetry of the problem, reducing the GLW functional to the respective functional for a tetrahedrally symmetric system with a two-component order parameter  $\varphi = \{\varphi_1, \varphi_2\}$ . Since the plane  $u_1 = u_2 \equiv u$  is an obvious integral of the initial system (1.6), on it the number of equations decreases still further:<sup>15</sup>

$$\frac{\partial u}{\partial l} = \varepsilon u - \frac{9}{2} u^2 - \frac{1}{2} v^2, \quad \frac{\partial v}{\partial l} = v(\varepsilon - 3u - 2v). \quad (1.9)$$

The phase portrait of this system is depicted in Fig. 1b. In addition to the two points  $\mu_1$  ( $u = v = \frac{1}{3}$ ) and fixed points are

clearly visible: the Ising point  $\mu_3(u = \frac{2}{3}, v = 0)$  and the Gaussian point  $\mu_0(u = v = 0)$ . Points  $\mu_2$  and  $\mu_3$  belong to the obvious separatrices  $v = 3u$  and  $v = 0$ , respectively. Since at  $u_1 = u_2 \equiv u$  the system possesses an additional symmetry under rotations of the vector  $\varphi$  by  $\frac{1}{4}\pi$ , these two separatrices are symmetry-coupled.<sup>17</sup> Indeed, the introduction of new variables  $\xi_1 = \varphi_1 + \varphi_2$  and  $\xi_2 = \varphi_1 - \varphi_2$  maps the function  $F(\varphi_1; \varphi_2)$  into a similar form in these variables, with the new parameters  $u_1$  and  $v_1$  related to the initial  $u$  and  $v$  as follows:

$$u_1 = \frac{u+v}{2}, \quad v_1 = \frac{3u-v}{2}. \quad (1.10)$$

Under the transformations (1.10) the separatrices  $v = 3u$  and  $v = 0$  change places; this is accompanied by a change in places of the minima and saddle points of the function, which lie on the axes of coordinates  $\varphi_1$  and  $\varphi_2$  and the diagonals  $\varphi_1 = \varphi_2$ . This transformation provides additional freedom in studying the system, which we use in what follows.

### 3. EVOLUTION OF THE FLUCTUATING ORDER PARAMETERS

As noted in the Introduction, the fact that phase trajectories leave the stability region is usually interpreted as a fluctuation-induced ‘‘collapse’’ of PT2 to PT1. It is well known, however, that PT1 is accompanied by nucleation and steady growth of the nuclei. Mathematically, the reason is the presence of a hump in the local free-energy density, a hump that separates energy-distinct local minima. But in the present case there is no such maximum. An approximate calculation of the partition function  $Z$  and the effective free energy having the desired maximum<sup>19–23</sup> does little to clarify the physics of the process, since in the final analysis the coarsening of the description because of the scaling RG transformations is also a distinctive method of calculating  $Z$ . At the same time we believe that, just as in the case of ordinary PT1 (see Ref. 29), nuclei emerge ‘‘by themselves’’ solely from fluctuation noise as soon as the parameters of the system are taken from the respective sector of the RG phase portrait.

To prove this, we write the equations for the relaxation of the fluctuating fields in the form

$$\frac{\partial \varphi_i}{\partial t} = - \frac{\delta \mathcal{H}}{\delta \varphi_i} + f_i(\mathbf{r}; t), \quad (2.1)$$

where  $\delta \mathcal{H} / \delta \varphi_i$  is the variational derivative of  $\mathcal{H}$ ,  $f_i(\mathbf{r}; t)$  is the delta-correlated white noise,

$$\langle f_i(\mathbf{r}; t) \rangle = 0, \quad \langle f_i(\mathbf{r}; t) f_j(\mathbf{r}'; t') \rangle = D \delta(t-t') \delta(\mathbf{r}-\mathbf{r}'), \quad (2.2)$$

and the kinetic coefficients are hidden in the renormalization of time and the parameters  $\kappa$ . Solving Eq. (2.1) numerically, we discovered that the RG method predicts such transition kinetics. The relevant results are given at the end of this section. We believe, however, that it is expedient first to discuss some qualitative (analytical) ideas concerning the structure of the expected solutions.

The fluctuations generated by the noise  $f$  relax, remaining for different amounts of time in different spatial configurations of  $\varphi_i(t; \mathbf{r})$ . They remain longest near attractor distributions, which correspond to some of the solutions of the static equations  $\delta \mathcal{H} / \delta \varphi_i = 0$ :

$$\nabla^2 \varphi_i = \frac{\partial F(\varphi_1; \varphi_2)}{\partial \varphi_i}. \quad (2.3)$$

In such configurations the energy density in the GLW functional is uniquely related to the local form  $F(\varphi_1; \varphi_2)$ . The validity of this statement can be demonstrated for an arbitrary nonlocal operator  $\varphi_i(\mathbf{r}) V_{ij}(\mathbf{r}-\mathbf{r}') \varphi_j(\mathbf{r}')$  replacing  $(\text{grad} \varphi_i)^2$  in the GLW functional, but the simplest way to do so is to use the one-dimensional version of Eq. (2.3a):

$$\frac{d^2 \varphi_i}{dx^2} = \frac{\partial F(\varphi_1; \varphi_2)}{\partial \varphi_i}. \quad (2.4)$$

Aside from its simplicity, this version is very useful for understanding, since it actually describes one-dimensional sections,  $d=1$ , of the three-dimensional distribution of  $\varphi$  in those regions of space  $\{\mathbf{r}\}$  in which all the components of the gradients are small except one. Numerical studies show that such configurations of the nonlinear excitations are typical for the majority of the points of  $\{\mathbf{r}\}$ . Employing Eq. (2.3b), we immediately get

$$\frac{1}{2} \frac{d}{dx} \left[ \left( \frac{d\varphi_1}{dx} \right)^2 + \left( \frac{d\varphi_2}{dx} \right)^2 \right] = \frac{\partial F}{\partial \varphi_1} \frac{d\varphi_1}{dx} + \frac{\partial F}{\partial \varphi_2} \frac{d\varphi_2}{dx} = \frac{dF}{dx},$$

whence

$$\frac{1}{2} [(\text{grad} \varphi_1)^2 + (\text{grad} \varphi_2)^2] = F(\varphi_1; \varphi_2) + \text{const}. \quad (2.5)$$

Here selection of the constant is determined by the magnitude and sign of parameters  $\kappa$ , primarily  $\tau_i$ . The fixed-sign gradient terms in the energy density yield a positive correction to this density. This effectively renormalizes  $\tau_i$ , in accordance with the known RG result. Thus, if we wish to observe the ordering process (even in the incomplete form, i.e., in the critical region), we must take  $\tau_i < 0$ . Since noise intensity is determined by the absolute temperature,  $D \propto T$

(here  $T \equiv 1$ ), to study the system behavior in the fluctuation region one must select  $-\tau_i \approx D \propto 1$ . The parameters can be chosen more precisely by direct numerical experiments.

When the  $\tau_i$  are negative, the typical excitations in the system are inhomogeneities of the domain-wall type. For such excitations the constant in (2.4) should be chosen equal to the value of  $-F(\varphi_1; \varphi_2)$  taken at the minima of this function:  $F(\varphi_1; \varphi_2) = F^{(0)}$ . As a result the energy correction related to the excitations and measured with respect to the equilibrium energy  $E^{(0)} = \int dx F^{(0)}$  has the form

$$E = \int dx \left[ \frac{(\text{grad} \varphi_1)^2 + (\text{grad} \varphi_2)^2}{2} + F(\varphi_1; \varphi_2) \right] - E^{(0)} = 2 \left[ \int dx F(\varphi_1; \varphi_2) - E^{(0)} \right]. \quad (2.6)$$

An approximate minimum of this energy is provided by the solutions of Eq. (2.3), or the configurations of  $\varphi$  close to these solutions, that minimize  $F(\varphi_1; \varphi_2)$  (for  $\varphi \neq \text{const}$ ). Such configurations may be expected to be, for one thing, the curves connecting the minimum points and passing either through the saddle point or through the maximum of  $F(\varphi_1; \varphi_2)$ . Direct modeling (Fig. 2a) shows that the distributions actually selected by the system are indeed close to such configurations (and practically only to such).

Further investigation requires fixing the range of the parameters  $u_i$  and  $v$ . For analytical calculations it is convenient to select a range of parameters corresponding to an advantageous mixed state, whereas for a graphic representation of the results of numerical calculations the situation involving only one ordered field is preferable. The possibility described above of inverting these two situations enables one to choose the cases without introducing further restrictions. Selecting  $u_1 u_2 > v^2$ , we use the following form of the approximate relationship between the  $\varphi_i$  fields:

$$\frac{\partial F}{\partial \varphi_i} = \tau_i + u_i \varphi_i^2 + v \varphi_{j \neq i}^2 \approx 0, \quad (2.7)$$

which is a good approximation of the desired domain walls. Equation (2.6) defines a family of second-order curves that are fragments of ellipses or hyperbolas, depending on the sign of  $v$ . Note that the curve  $v=0$  is a separatrix of the RG equations. We wish to show now that this curve also separates the respective nonlinear excitations into two levels advantageousness. Using (2.6) as an equality, we solve it for  $\varphi_1$ ,

$$\varphi_1^2 = - \frac{\tau_1 + v \varphi_2^2}{u_1}, \quad (2.8)$$

and integrate the equation for  $\varphi_2$ . We have

$$\frac{d^2 \varphi_2}{dx^2} = \varphi_2 \frac{(u_1 \tau_1 - v \tau_1) + (u_1 u_2 - v^2) \varphi_2^2}{u_1}. \quad (2.9)$$

Bearing in mind that  $u_1 \tau_2 - v \tau_1 < 0$  and  $u_1 u_2 - v^2 > 0$ , we obtain

$$\varphi_2 = \sqrt{\frac{v \tau_1 - u_1 \tau_2}{u_1 u_2 - v^2}} \tanh x \sqrt{\frac{v \tau_1 - u_1 \tau_2}{2 u_1}}. \quad (2.9a)$$

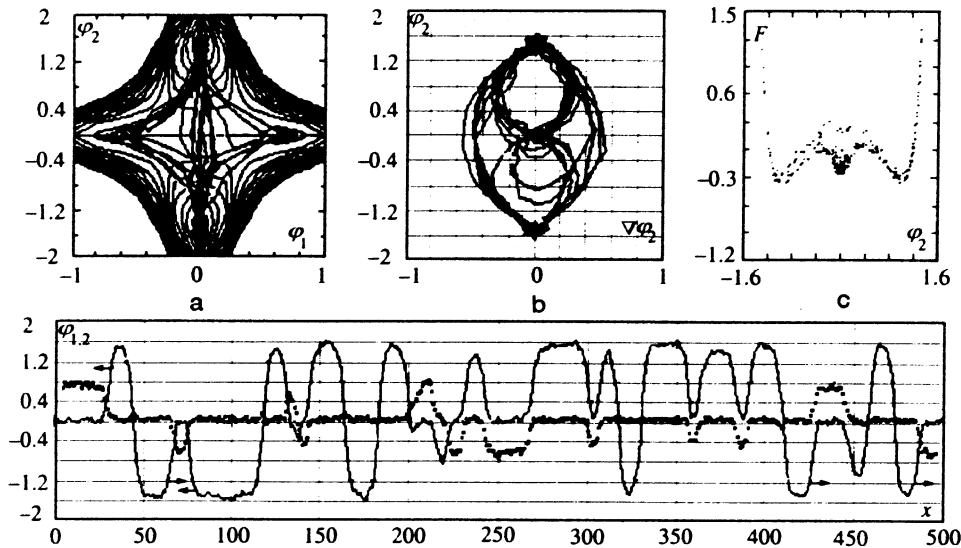


FIG. 2. One-dimensional sections of the distributions of the fields  $\varphi_1$  (dotted curve) and  $\varphi_2$  (solid curve) ( $u_1=0.2$ ,  $u_2=1$ , and  $v=5$ ). The arrows point in the direction of the movement of the new-phase domain walls. The insets depict the following: (a) the phase portrait as projected on the  $(\varphi_1, \varphi_2)$  (hyper-)plane and showed against the background of the level curves of surface  $F(\varphi_1; \varphi_2)$ , (b) the same as projected on the  $(\text{grad}\varphi_2, \varphi_2)$  plane, and (c) the energy density  $\bar{F}$  in the GLW functional as a function of  $\varphi_2$  (the projection on the  $(\bar{F}, \varphi_2)$  plane).

In the vicinity of the bisector  $u_1 \approx u_2 = u$  and, respectively,  $\tau_1 \approx \tau_2 = \tau$  this solution degenerates into

$$\varphi_2 = \sqrt{-\frac{\tau}{u+v}} \tanh x \sqrt{\frac{\tau(v-u)}{2u}}. \quad (2.9b)$$

The solutions (2.9) coincide with the well-known domain walls for a one-component order parameter, provided that the quantities are properly renormalized, while the nontrivial (in this sense) variation of the second component is determined by Eq. (2.7).

Now we compare the contributions to the energy from the various sequences of signs of both fields,  $\varphi_1$  and  $\varphi_2$ : when they both flip (case  $\alpha$ ), that is, in the  $(\varphi_1, \varphi_2)$  plane the domain wall passes through the point  $\varphi_1 = \varphi_2 = 0$ , and when each rotates successively (case  $\beta$ ), that is, for two walls of the (2.9b) type. Direct substitution and simple algebraic transformations yield, respectively,

$$E^{(\alpha)} - E^{(0\alpha)} = (u+v) \int dx (\varphi^2 - \varphi_0^2)^2, \quad (2.10a)$$

with  $\varphi_0^2 = -\tau/(u+v)$  and  $\varphi = \varphi(x\sqrt{-\tau/2})$ , and

$$E^{(\beta)} - E^{(0\beta)} = \sqrt{(u-v)/u} (E^{(\alpha)} - E^{(0\alpha)}), \quad (2.10b)$$

where we have allowed for the fact that the functional dependence of the  $\varphi_i$  on the spatial coordinates coincide for the two cases to within the substitution  $x \rightarrow \bar{x}\sqrt{(u-v)/u}$ , for which we have introduced the change of variables  $\int dx \rightarrow \int d\bar{x}\sqrt{(u-v)/u}$  in case  $\beta$ . Equation (2.10b) clearly shows that for  $v > 0$  the total energy of a pair of respective excitations is higher than the energy of each excitation, while for  $v < 0$  the situation is the opposite. In other words, the separatrix that on the phase portrait isolates different types of critical behavior also distinguishes nonlinear excitations of different levels of advantageousness in the system. In the final analysis it is the disadvantageousness of excitations of the 90-degree domain-wall type that makes nucleation inevitable when the system becomes ordered in the  $v < 0$  region.

To illustrate the phenomenology of this process numerically, it is convenient, as mentioned earlier, to use the region

$v > 3u$  instead of  $v < 0$ . Qualitatively the picture is as follows. In an early stage of the evolution, when only terms linear in  $\varphi_i$  operate in Eqs. (2.1), both fields fluctuate correlation-free and on an equal basis. The spikes of the field  $\varphi_1$  reach the vicinity of their minimum points  $\pm\varphi_{10}$  before those of  $\varphi_2$  reach  $\pm\varphi_{20}$  (for the sake of definiteness, here and in what follows  $u_1 > u_2$ , i.e.,  $\varphi_{10} < \varphi_{20}$ ). But as  $\varphi$  grows, the correlation between the fluctuations of each of the fields and between different fields comes into play. Since final ordering of field  $\varphi_2$  is more advantageous, the system tends to broaden the regions with  $\varphi_2 \neq 0$  at the expense of  $\varphi_1$ . But the spikes of  $\varphi_1$  are very close to the points  $\pm\varphi_{10}$  and are pinned, so to say, to the local minima in their vicinity. At the same time, the compromise walls, making contact with  $\varphi_1$  during flips of  $\varphi_2$ , are not advantageous and the system tends to completely eradicate regions with  $\varphi_1 \neq 0$ . As a result in the intermediate kinetic stage of the evolution to equilibrium there appears a state with nuclei of phase  $\varphi_2$  that “viscously” expand in the field of fluctuations of  $\varphi_1$ . For a one-dimensional section of  $\varphi_{1,2}$  along  $x$  this process is illustrated by Fig. 2. Here the insets (a) and (b) show the projections of the phase portrait of the system on the  $(\varphi_1, \varphi_2)$  and  $(\text{grad}\varphi_2, \varphi_2)$  hyperplanes, respectively. The pinning regions of  $\varphi_1$  are clearly seen in Fig. 2a, as well as the attractor structure in Fig. 2b typical of PT1 and corresponding to the moving new-phase domain walls, a result recently obtained in Ref. 29. We note once more that, in contrast to the standard case,<sup>29</sup> the situation here is such that the formation of steadily moving domain walls occurs in the absence of barriers in the local density  $F(\varphi_1; \varphi_2)$ . More precisely, in reality such barriers emerge because of the specific route that the system takes to equilibrium in the four-dimensional space  $\{\varphi_1, \varphi_2, \text{grad}\varphi_1, \text{grad}\varphi_2\}$ . The barriers can be visualized by formally projecting the GLW-functional density

$$\begin{aligned} \bar{F}(\varphi_1, \varphi_2, \text{grad}\varphi_1, \text{grad}\varphi_2) = & \frac{1}{2}[(\text{grad}\varphi_1)^2 + (\text{grad}\varphi_2)^2] \\ & + F(\varphi_1; \varphi_2) \end{aligned} \quad (2.11)$$

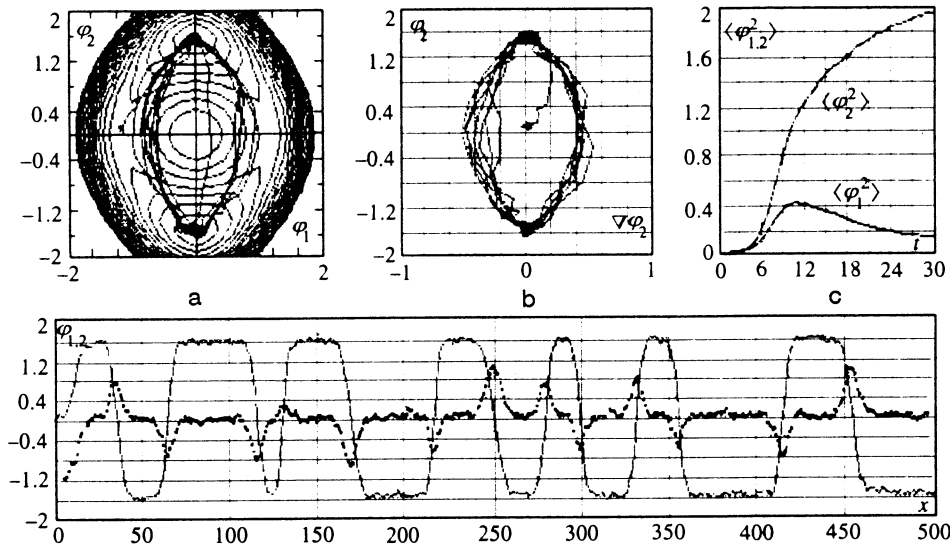


FIG. 3. As in Fig. 2 for  $v < 3\sqrt{u_1 u_2}$  ( $u_1 = 0.2$ ,  $u_2 = 0.4$ , and  $v = 0.4$ ). The inset (c) depicts the temporal evolution of the mean squares of the fields  $\varphi_i$ .

at each point of array  $x$  on the  $(\bar{F}, \varphi_2)$  plane, as is done in the inset (c) to Fig. 2.

For the sake of comparison, a similar picture of a fairly late stage in the ordering process for the case where  $v < 3u$  is depicted in Fig. 3 and the insets (a) and (b) to it. Clearly, there are no steadily moving walls, and to each flip of  $\varphi_2$  there corresponds a local spike in  $\varphi_1$ . Inset (c) in Fig. 3 depicts the temporal evolution of the mean squares of the  $\varphi_i$ . Clearly visible is the stage of their regular growth, which is the longer the deeper the system is fixed in the critical region of parameters  $\tau$  and  $D$ . In this stage their correlation functions (Fig. 4a) have practically the same halfwidth  $\Gamma$  that increases with time as  $\Gamma \propto \sqrt{t}$  (Fig. 4b), which corresponds, on the one hand, to the growth of the characteristic size of on-the-average ordered regions and, on the other, to the growth of the correlation range  $r_c$  in accordance with the Ornstein-Zernike equation. In Refs. 31 and 32 this stage has been studied in greater detail for the cases of a scalar order parameter and a PT2 or spinodal decomposition.

If the parameters are such that the system never freezes in the ordered state, then regular fluctuations, apparently, correspond to the case of asymptotic symmetry described in the previous section. But if the system becomes ordered, at a fairly late stage the  $\langle \varphi_1^2 \rangle$  and  $\langle \varphi_2^2 \rangle$  split. The same is true of the areas occupied by regions with order of basically the  $\varphi_1$  or  $\varphi_2$  type. Since, however, 90-degree walls here are advantageous, the ordering regions are usually redistributed via temporal flattening-out of the respective sections of the boundaries, that is, through minimum gradient contributions to the energy. As a result, no effective barriers appear and the transition remains of the PT2 type, as predicted by the mean-field theory.

We performed computer simulations of the evolution of two-dimensional sections of the fluctuating fields for both cases,  $v > 3u$  and  $v < 3u$ , using  $140 \times 140$  arrays. Figures 5 and 6 each depict two typical stages in the evolution. The various levels of  $\varphi_1$  and  $\varphi_2$  normalized to their maximum values for each instantaneous distribution and time (insets (a. i) and (b. i)) are shown by gradations of gray. A uniformly gray color corresponds to  $\varphi_i \approx 0$ , while dark and light spots

correspond to positive and negative values of the  $\varphi_i$ . Figs. 5.a.1 and 6.b.2 are the most characteristic here. The first shows for  $v > 3u$  the distribution of circular ("spherical") nuclei  $\varphi_2 \neq 0$  of both signs, whose growth is damped by the presence of fluctuations of the second field. Figure 6.b.2 illustrates the final stage in the evolution of the system for

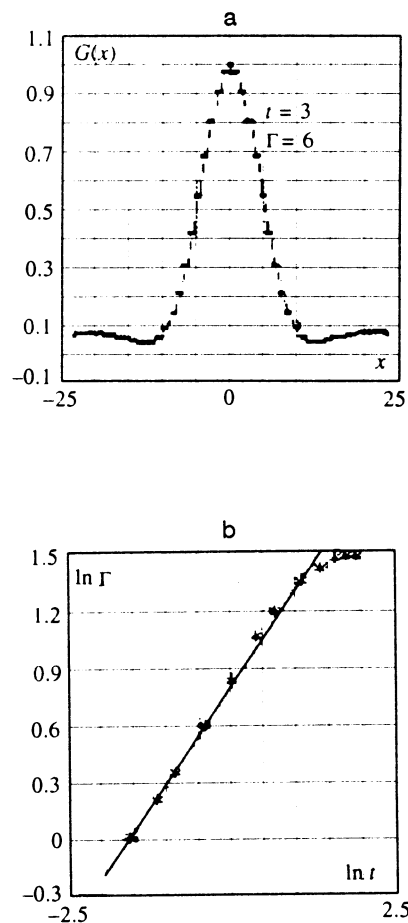


FIG. 4. The correlation function  $G(x)$  of fluctuations of  $\varphi_2$ : (a) the dependence of  $G(x)$  on the spatial coordinate, and (b) the temporal evolution of the halfwidth  $\Gamma$ .

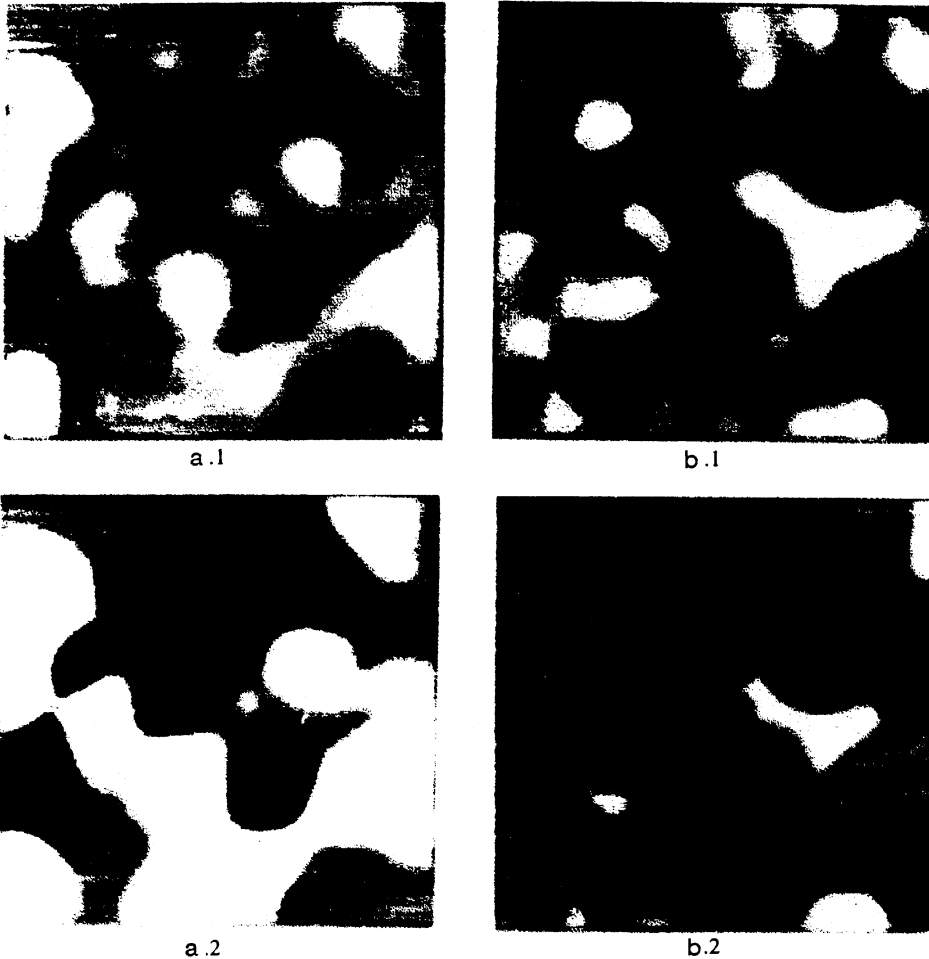


FIG. 5. Distributions of the densities of  $\varphi_1$  and  $\varphi_2$  ((a) and (b), respectively) for different times ((a.1,2) and (b.1,2), respectively) for  $v > 3\sqrt{u_1 u_2}$ .

$v < 3u$ , when initially equitable domains with  $\varphi_1 \neq 0$  form “thick” structured walls between the domains with  $\varphi_2 = 0$ . These walls partially repeat the initial corrugated structure of the fluctuating field  $\varphi_1$  depicted in Fig. 6.b.1. It is clear that the respective stage in the evolution with  $v > 3u$  depicted in Figs. 5.a.2 and 5.b.2 differs from this picture in that the strongly pronounced nuclei of field  $\varphi_2$  coalesce and completely expel the regions with  $\varphi_1 \neq 0$ .

Normalizing the gradations of gray to the peak values of  $\varphi_i$  reveals the fine structure of the densities but somewhat masks the dramatic difference between the two cases. In view of this, for the stages depicted in the portions a.1 and b.1, Figs. 7a and 7b depict, respectively, the distributions of the sum of squares,  $\varphi^2 = \varphi_1^2 + \varphi_2^2$ , for  $v > 3u$  and  $v < 3u$ , respectively. Clearly, for  $v > 3u$  there are well-developed single spikes in the density of  $\varphi^2$ , while for  $v < 3u$  there are spread-out regions (dark spots) where  $\varphi^2$  is quite uniformly nonzero, separated by comparatively narrow boundaries  $\varphi^2 \approx 0$  (light regions).

Concluding this section, we make some comments concerning Fig. 6.b.2. The structured boundaries in this figure are also the domains  $\pm \varphi_1$  (black and white, respectively). Their walls, intersecting the boundaries  $\varphi_2 = 0$ , form punctures in which the total  $\varphi^2 = \varphi_1^2 + \varphi_2^2$  vanishes. If  $u_1 = u_2 = v$ , the difference between the two types of domains vanishes and the respective punctures become isolated singularity points of the absolute value of the two-component

order parameter  $\varphi = (\varphi_1, \varphi_2)$ . For the isotropic  $O_2$  model, both the RG method and the kinetic approach employed here predict trivial behavior in the ordering process. Usually, however, one does not encounter behavior of the  $O_2$  universality class in real systems. For instance, in the classical example of this type of GLW functionals, which describes the transition to superconductivity, there is a relation between the order parameter  $\varphi$  and the indestructible fluctuations of the (gauge) electromagnetic field. The fact that the two are related leads to fluctuation-induced PT1, which we discuss in the next section.

#### 4. NUCLEATION IN THE TRANSITION TO SUPERCONDUCTIVITY

The punctures in the absolute value of the order parameter, situated at the intersections of the lines on which the separate components of the order parameter vanish, act as nonlinear vortex excitations. In the final analysis, the origin of such excitations lies in the statistically independent fluctuation of the components of the order parameter. Such excitations can easily be visualized, for instance, by forming the combination  $\varphi_1 \text{grad} \varphi_2 - \varphi_2 \text{grad} \varphi_1$ , the analog of the quantum current for the complex-valued function  $\psi = \varphi_1 + i\varphi_2$ . In a superconductor with its complex-valued

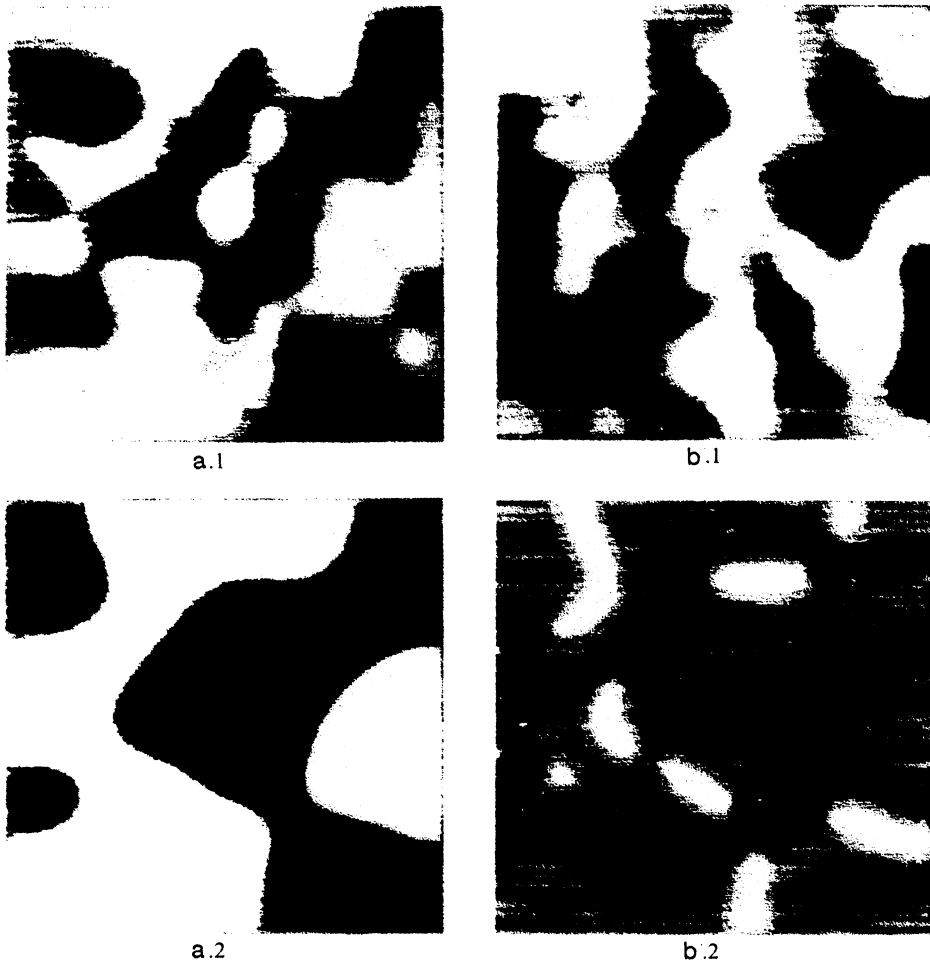


FIG. 6. As in Fig. 5 for  $v < 3\sqrt{u_1 u_2}$ .

order parameter, such a construction acquires physical meaning, and these nonlinear excitations greatly affect the thermodynamics of the entire system.

The fact that the vortex configurations of the order parameter play an important role in the kinetics of the phase transition to superconductivity is well known. An especially large number of studies of such configurations were carried out with flat and quasi-two-dimensional systems of finite thickness. For instance, for a flat superconductor, to which the Mermin–Wagner–Hohenberg theorem on the inhibition of long-range order by strong fluctuations<sup>34</sup> can be applied, the presence of a phase transition is related to the formation of vortex–antivortex pairs and their possible unpairing in certain conditions.<sup>35–37</sup> The concept of vortex pairs, brought into the picture to explain the phase transition in two-dimensional superconductors, has been corroborated in many experiments. Also well-known are analytical vortex-like solutions for a superconductor in an external field (Abrikosov vortices).<sup>38</sup> Such solutions cannot be obtained by analytical means in the absence of an external field. The main difficulty is that from the very beginning the coordinated evolution of the order parameter and the vector potential in a vortex pair have to be considered. Here, since the vortices forming a pair attract each other, such a solution can exist only dynamically, so that to obtain the solution one cannot, in principle, resort only to an equation resulting from setting the variation of the free energy to zero.

The GLW functional for a superconductor has the form

$$\mathcal{H} = \mathcal{H}_0 + \int d^d r \{ c |(\nabla - ig\mathbf{A})\psi|^2 + \alpha |\psi|^2 + \frac{1}{2}\beta |\psi|^4 + \vartheta (\text{curl}\mathbf{A})^2 \}, \quad (3.1)$$

where  $\psi = \varphi_1 + i\varphi_2$  is the complex-valued order parameter,  $\mathbf{A}$  is the (gauge) vector potential,  $d$  is the dimensionality of the space,  $c = \hbar^2/4m$ ,  $g = 2e/\hbar c$ ,  $\vartheta = \frac{1}{8}\pi$ , and  $\alpha \sim (T - T_c)$  and  $\beta$  are phenomenological constants.

It is customary to assume that the fields  $\varphi_1$ ,  $\varphi_2$ , and  $\mathbf{A}$  fluctuate independently. In other words, the partition function  $Z$  with the functional (3.1) must be integrated independently with respect to each field. Following Ref. 33, we show that integration of  $Z$  over the fluctuations of the gauge electromagnetic field (i.e., with respect to  $\mathbf{A}$ ) leads to an effective GL functional characteristic of a PT1.

If the Ginzburg parameter for the given system is extremely small and we can ignore the interaction of fluctuations of field  $\psi$  (as is the case with a good type I superconductor), integrating  $Z$  with respect to  $\mathbf{A}$  directly, we get an effective GLW functional determined by the following relation:

$$\exp \{ -F_{\text{eff}}(\psi) \} = \int D\mathbf{A} \exp \{ -\mathcal{H}(\psi; \mathbf{A}) \}. \quad (3.2)$$

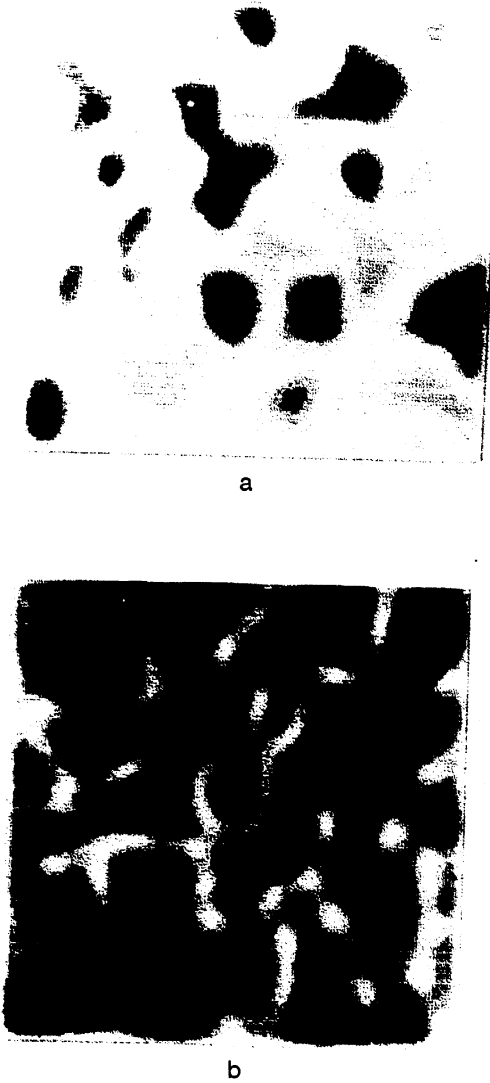


FIG. 7. (a) and (b): Distributions of the density of  $\varphi^2 = \varphi_1^2 + \varphi_2^2$  for the configurations depicted in Figs. 5.(a,b).1 and 6.(a,b).1, respectively.

This leads to a change in the coefficient  $\alpha$  of the term quadratic in  $\psi$  in Eq. (3.1):

$$\alpha \rightarrow \alpha + cg^2 \langle \mathbf{A}^2 \rangle_\psi. \quad (3.3)$$

The average can easily be calculated by perturbation theory in  $\psi$ , and in the lowest orders has the form

$$\langle \mathbf{A}^2 \rangle_\psi = \frac{1}{2\vartheta\pi^2} - \sqrt{\frac{4cg^2}{\vartheta}} \frac{|\psi|}{8\pi\vartheta}. \quad (3.4)$$

Here the first term simply renormalizes the critical temperature, while the second adds the correction  $\propto |\psi|^3$  to the GLW function, whose presence signals that we are dealing with a PT1 in the system.

But if the fluctuations of field  $\psi$  are considerable in a broader region, as is the case for high- $T_c$  systems, we must study the RG equations for the vertices of functional (3.1). Usually in such systems the order parameter  $\psi$  has ( $n > 2$ ) components. Halperin, Lubensky, and Ma<sup>33</sup> set up and studied the RG equation for such an isotropic functional and showed that for a finite charge ( $g \neq 0$ ) these equations have a fixed point only for a clearly unphysical value of  $n$  greater

than 731.8. Here we do not write these equations, since for real systems with a broad fluctuation region the situation is, possibly, still more complicated owing to nontrivial pairing. The latter leads to the appearance in the GLW functional of anisotropic invariants, and the continuous phase transition irrevocably collapses to a PT1, irrespective of such a subtle effect as the interaction with the fluctuations of the gauge electromagnetic field (see, e.g., Ref. 39 for a review). But the objective of this section is, after all, to establish the vortex nature of nuclei for the transition in an isotropic system.

The equations of motion for the components of the order parameter follow from the generalized GL equation and in the general case have the form

$$\frac{1}{\gamma_1} \frac{\partial \varphi_1}{\partial t} = c \nabla^2 \varphi_1 + cg(2\mathbf{A} \cdot \text{grad} \varphi_2 + \varphi_2 \text{div} \mathbf{A}) - \varphi_1 [(\alpha + cg^2 \mathbf{A}^2) + \beta(\varphi_1^2 + \varphi_2^2)] + f_1(\mathbf{r}, t), \quad (3.5a)$$

$$\frac{1}{\gamma_2} \frac{\partial \varphi_2}{\partial t} = c \nabla^2 \varphi_2 - cg(2\mathbf{A} \cdot \text{grad} \varphi_1 + \varphi_1 \text{div} \mathbf{A}) - \varphi_2 [(\alpha + cg^2 \mathbf{A}^2) + \beta(\varphi_1^2 + \varphi_2^2)] + f_2(\mathbf{r}, t), \quad (3.5b)$$

$$\frac{1}{\gamma_3} \frac{\partial \mathbf{A}}{\partial t} = \vartheta [\nabla^2 \mathbf{A} - \text{grad}(\text{div} \mathbf{A})] + cg(\varphi_1 \text{grad} \varphi_2 - \varphi_2 \text{grad} \varphi_1) - cg^2 \mathbf{A}(\varphi_1^2 + \varphi_2^2) + f_3(\mathbf{r}, t). \quad (3.5c)$$

Here  $\gamma_1 = \gamma_2$  are relaxation constants, and  $f_i(\mathbf{r}, t)$  is noise. In order to clarify the physical meaning of the additional equation (3.5c), we note that the total current density  $J$  in the superconductor is  $J_n + J_s = (c/4\pi) \text{curl} \text{curl} \mathbf{A}$ . The supercurrent density  $J_s$  is defined as  $J_s = cg(\varphi_1 \text{grad} \varphi_2 - \varphi_2 \text{grad} \varphi_1) - cg^2 \mathbf{A}(\varphi_1^2 + \varphi_2^2)$ , and the normal-current density  $J_n$  is  $\sigma E = -\sigma(\partial \mathbf{A} / \partial t)$ . Thus, Eq. (3.5c) determines the normal current in a superconductor, and the constant  $\gamma_3^{-1}$  is physically the normal electrical conductivity ( $\gamma_3^{-1} \sim T_c \tau_r$ , with  $\tau_r$  the relaxation time).<sup>40,41</sup>

Calculations were carried out on a flat grid of  $110 \times 110$  cells. The results obtained in this manner, as well as those of Sec. 2, should be interpreted as mere two-dimensional sections of three-dimensional distributions of the quantities in those regions of space where the dependence of these quantities on the  $z$ -coordinate is fairly weak. The initial conditions were chosen in different ways depending on the modeling scenario. Since the main idea of this section is to demonstrate the spontaneous creation of vortex pairs in the event of relaxation of the order parameter, the most striking within this context are the results obtained at zero initial conditions for  $\varphi_{1,2}$ .

A typical intermediate configuration obtained in the process of ordering of a type II superconductor ( $\kappa > \sqrt{1/2}$ ) is depicted in Fig. 8. Gradations of brightness in the separate parts of this figure ((a)–(d)) represent the values of the components of the order parameter (with medium gray representing the lines on which these components vanish), the distribution of the current density  $J_s$ , and the local magnetic field. Since we experimented with a system describing the transition both with an external magnetic field  $H$  and without one ( $H \neq 0$ ) and intended to comment on the processes taking

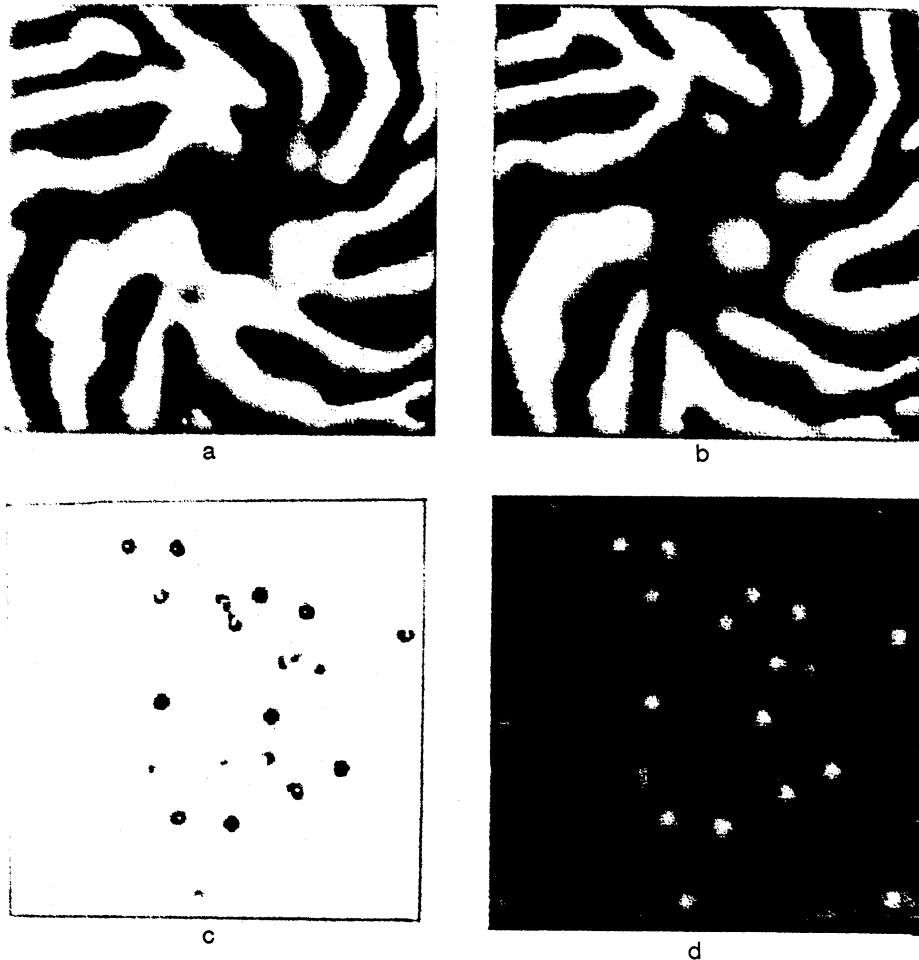


FIG. 8. Distributions of the densities of  $\varphi_1$  and  $\varphi_2$  obtained from Eqs. (3.5) ((a) and (b), respectively), and the distributions, correlated with the intersections of the lines of zero  $\varphi_1$  and  $\varphi_2$ , of the current density  $J_s$  (c) and the magnetic field (d) of the vortices directed along (bright spikes) and against (dark spikes) the external magnetic field ( $H=0.015$  in dimensionless units).

place in both cases, Fig. 8 depicts the densities of the respective quantities at low but finite  $H$  (the field is expelled from the sample in the transition).

There is convincing evidence that the cause of creation of vortex pairs is the statistically independent fluctuation of the components of the order parameter, as a result of which the regions in which these components are essentially non-zero do not overlap completely. Because of a phase difference, a (quantum) supercurrent, which generates a magnetic field, is created in such configurations. Interacting with the order parameter, this field, in turn, both makes the order parameter smaller and facilitates penetration of the sample by the (gauge) magnetic field where the order parameter is already small, that is, at the intersections of the lines of zero  $\varphi_1$  and  $\varphi_2$ . Figure 8c shows that the distribution of the total current density about the lines of magnetic flux is truly of a vortex type and corresponds to the intuitive idea of current distribution in vortex-antivortex pairs. Further evolution of these formations also agrees with accepted ideas: vortices attract each other and, in the process, merge and finally disappear. What is interesting is that ordinary terms "annihilation" and "collapse" do not quite convey the proper meaning. Most likely we are dealing simply with the damping of vortex-antivortex pair currents in a region with a reduced order parameter in the final stage of the merging of vortices. If the transition occurs in a field  $H \neq 0$ , in the course of the process an imbalance develops towards retaining a greater

number of vortices that are directed along the external field (as Fig. 8d clearly shows) and contain magnetic flux. Taking into account the same brightness, size, and stability of development of such formations in Fig. 8d, we note the universality and the attractor nature of the respective vortices of the superconductivity current. It is easy to incorporate inhomogeneities (of the "random-temperature" type, for instance) in the system of equations (3.5) and "pin" the resulting vortices. This offers broad possibilities for modeling mixed states, which, however, lies outside the scope of the present investigation.

When all three measurements have an equal status, the pair of volume globules of the uncorrelated components of the order parameter leads to the formation of a toroidal magnetic flux and has an effect on the thermodynamics of the system, determining the critical sizes of nuclei. Mutual attraction of the vortices and antivortices in pairs generated by order-parameter fluctuations (or compression of the toroidal magnetic flux at  $d=3$ ) creates an energy barrier leading to threshold nucleation. Since the interaction of vortices falls off as the distance between them increases ( $\propto 1/r^\alpha$ , where  $\alpha > 0$ ) and the gain in the nucleus energy grows in proportion to the nucleus volume ( $\propto r^d$ ), a nucleus has a certain critical size from which the nucleus inflates in space without limit. Smaller formations are certain to collapse. The relation between order-parameter fluctuations and vortex excitations gives the sought phenomenological explanation of the state-

ment that the phase transition to superconductivity always occurs as a first-order phase transition.

We are grateful to T. K. Soboleva, A. V. Radievski, and Yu. E. Kuzovlev for their valuable remarks, which improved the paper. One of the authors (A.É.F.) would like to thank Prof. J.-P. Badioli for hospitality and for the discussions of the theory of nucleation during their joint work at the University of Pierre and Marie Curie (Paris VI).

This work was partially supported within the "Pin" contest project of the Ukrainian State Committee for Science and Technology, and by the Soros International Science Foundation.

- <sup>1</sup>L. P. Kadanoff, *Physics* **2**, 263 (1966).
- <sup>2</sup>K. G. Wilson, *Phys. Rev. B* **4**, 3174 (1971).
- <sup>3</sup>K. Wilson and J. Kogut, *The Renormalization Group and the  $\epsilon$ -Expansion*, Wiley, New York (1974).
- <sup>4</sup>S. G. Gorishny, S. A. Larin, and F. V. Tkachov, *Phys. Lett. A* **101**, 120 (1976).
- <sup>5</sup>G. R. Golner and E. K. Reidel, *Phys. Rev. Lett.* **34**, 856 (1975).
- <sup>6</sup>L. J. C. Guillou and J. Zinn-Justin, *Phys. Rev. Lett.* **39**, 95 (1977).
- <sup>7</sup>I. F. Lyuksyutov, V. L. Pokrovski, and D. E. Khmel'nitski, *Zh. Eksp. Teor. Fiz.* **69**, 1817 (1975) [*Sov. Phys. JETP* **42**, 923 (1975)].
- <sup>8</sup>A. I. Sokolov and A. K. Tagantsev, *Zh. Eksp. Teor. Fiz.* **76**, 181 (1979) [*Sov. Phys. JETP* **49**, 92 (1979)].
- <sup>9</sup>P. Bak, D. Mukamel, and S. Krinsky, *Phys. Rev. B* **13**, 5065 (1975).
- <sup>10</sup>P. Bak, S. Krinsky, and D. Mukamel, *Phys. Rev. Lett.* **36**, 52 (1976).
- <sup>11</sup>A. Aharony, in *Phase Transitions and Critical Phenomena*, Vol. 6, edited by C. Domb and M. S. Green, Academic Press, New York (1977), p. 358.
- <sup>12</sup>M. Kerzberg and D. Mukamel, *Phys. Rev. B* **23**, 3943 (1978).
- <sup>13</sup>J. M. Kosterlitz, D. R. Nelson, and M. E. Fisher, *Phys. Rev. B* **13**, 412 (1976).
- <sup>14</sup>Yu. M. Ivanchenko, A. A. Lisyanski, and A. É. Filippov, *Zh. Eksp. Teor. Fiz.* **87**, 1019 (1984) [*Sov. Phys. JETP* **60**, 582 (1984)].
- <sup>15</sup>S. Ma, *Modern Theory of Critical Phenomena*, Addison-Wesley, Reading, Mass. (1976).
- <sup>16</sup>A. Z. Patashinski and V. L. Pokrovski, *Fluctuation Theory of Phase Transitions*, Pergamon Press, Oxford (1979).
- <sup>17</sup>Yu. M. Ivanchenko, A. A. Lisyanski, and A. É. Filippov, *Fluctuation Effects in Systems with Competing Interactions*, Naukova Dumka, Kiev (1989) [in Russian].
- <sup>18</sup>N. N. Bogoliubov and D. V. Shirkov, *Introduction to the Theory of Quantized Fields*, 4th ed., Nauka, Moscow (1985) [in Russian]; an earlier edition of this book was translated at Wiley, New York, in 1979.
- <sup>19</sup>H. H. Jacobson and D. J. Amit, *Ann. Phys.* **133**, 57 (1981).
- <sup>20</sup>I. F. Lyuksyutov and V. L. Pokrovski, *Pis'ma Zh. Eksp. Teor. Fiz.* **21**, 22 (1975) [*JETP Lett.* **21**, 9 (1975)].
- <sup>21</sup>A. I. Sokolov, *Zh. Eksp. Teor. Fiz.* **84**, 1373 (1983) [*Sov. Phys. JETP* **57**, 798 (1983)].
- <sup>22</sup>J. Rudnick, *Phys. Rev. B* **18**, 1406 (1978).
- <sup>23</sup>Yu. M. Ivanchenko, A. A. Lisyanski, and A. É. Filippov, *Phys. Lett. A* **119**, 55 (1986).
- <sup>24</sup>A. É. Filippov, *Teoret. Mat. Fiz.* **91**, 320 (1992).
- <sup>25</sup>J. Rudnick, *Phys. Rev. Lett.* **34**, 438 (1975).
- <sup>26</sup>P. Shukla and M. S. Green, *Phys. Rev. Lett.* **34**, 436 (1975).
- <sup>27</sup>S. A. Breus and A. E. Filippov, *Physica A* **192**, 486 (1993).
- <sup>28</sup>Yu. M. Ivanchenko, A. E. Filippov, and A. V. Radievsky, *J. Stat. Phys.* **71**, 1003 (1993).
- <sup>29</sup>Yu. E. Kuzovlev, T. K. Soboleva, and A. É. Filippov, *Zh. Eksp. Teor. Fiz.* **103**, 1742 (1993) [*JETP* **76**, 858 (1993)].
- <sup>30</sup>Yu. E. Kuzovlev, T. K. Soboleva, and A. É. Filippov, *Pis'ma Zh. Eksp. Teor. Fiz.* **58**, 353 (1993) [*JETP Lett.* **58**, 357 (1993)].
- <sup>31</sup>T. M. Rogers, K. R. Elder, and R. C. Desai, *Phys. Rev. B* **37**, 9638 (1988).
- <sup>32</sup>K. R. Elder and R. C. Desai, *Phys. Rev. B* **40**, 243 (1989).
- <sup>33</sup>B. I. Halperin, T. C. Lubensky, and S. Ma, *Phys. Rev. Lett.* **32**, 292 (1974).
- <sup>34</sup>N. D. Mermin and H. Wagner, *Phys. Rev. Lett.* **17**, 1133 (1966); P. C. Hohenberg, *Phys. Rev.* **158**, 383 (1967).
- <sup>35</sup>V. L. Berezinski, *Zh. Eksp. Teor. Fiz.* **59**, 907 (1970) [*Sov. Phys. JETP* **32**, 493 (1971)]; **61**, 1144 (1971) [**34**, 610 (1972)].
- <sup>36</sup>J. M. Kosterlitz and D. J. Thouless, *J. Phys. C* **6**, 1181 (1973).
- <sup>37</sup>J. M. Kosterlitz, *J. Phys. C* **7**, 1046 (1974).
- <sup>38</sup>A. A. Abrikosov, *Modern Theory of Metals*, North-Holland, Amsterdam (1990).
- <sup>39</sup>D. I. Uzunov, in *Advances in Theoretical Physics*, edited by E. R. Caianello, World Scientific, Singapore (1990), p. 96.
- <sup>40</sup>H. Frahm, S. Ullah, and A. T. Dorsey, *Phys. Rev. Lett.* **66**, 3067 (1991).
- <sup>41</sup>F. Liu, M. Mondello, and N. Goldenfeld, *Phys. Rev. Lett.* **66**, 3071 (1991).

Translated by Eugene Yankovsky

This article was translated in Russian. It is reproduced here the way it was submitted by the translator, except for stylistic changes by the Translation Editor.